ISSN: 2710-0723

Investigation of Energy Recovery Potential and Control Performance in Energy-Regenerative Suspension Systems with Inter-Axle Preview Control

Tianliang Wu*

School of Mechanical and Power Engineering, Henan Polytechnic University, Henan, China

*Corresponding Author

Abstract

This paper studies a novel active control method for vehicle energy-regenerative suspension systems. The suspension system can absorb road impacts to enhance vehicle comfort and safety. In conventional suspension systems, dampers dissipate kinetic energy during shock absorption. By employing a linear motor as the vibration energy harvester, the proposed system enables energy recovery while functioning as an active actuator to improve performance when required. This research designs an Inter-Axle Preview-Enhanced Model Predictive Control for Energy-Regenerative Suspension Systems based on inter-axle preview theory. A Four-Degree-of-Freedom 1/2 vehicle Suspension Dynamics Model is established for the energy-regenerative suspension system. The Model Predictive Control is enhanced using the inter-axle preview method. An analysis is conducted on the two control modes. In Active Control Mode, the system generates active actuation force to enhance suspension dynamics performance. In Self-Powered Control Mode, the front axle system operates as a vibration energy harvester to power the rear axle active actuator. Simulation analyses evaluate the control strategy's dynamic performance and application potential in suspension systems. The results show that the system studied in this paper can improve the vehicle system dynamics performance. It has development potential and application value in active control and energy regeneration.

Keywords

Vehicle System Dynamics; Active Suspension; Energy Regenerative Suspension; Model Predict Control.

1. Introduction

Intelligent vehicles, as a complex that can actively perceive the environment, optimize decisions in real time, and have multi-level assisted driving capabilities, have higher requirements for suspensions. The ideal intelligent suspension is capable of actively suppressing road impacts by referring to the real-time vehicle status information and environmental information provided by multi-modal sensors.[1,2] It can meet the modeling requirements of intelligent control algorithms for vehicle systems and roads, providing more feedback information and system status. It can also collaborate with driving assistance systems to offer active force assistance for adjusting the body posture in multiple operating conditions such as autonomous driving, steering, and braking[3].

This paper studies a suspension system that has the functions of passively recovering vibration energy, actively suppressing vehicle body vibrations, collecting and processing road information, and predicting road models, which can contribute to the intelligence of vehicles.

The energy-regenerative suspension can recover the energy dissipated to absorb road impacts. To counteract the adverse effects of road irregularities on system dynamic performance,

ISSN: 2710-0723

vehicles require additional energy consumption. Recovering this portion of energy contributes to extending vehicle range and enhancing energy utilization efficiency. Energy-regenerative suspensions exhibit diverse structural designs.[4,5] This study employs a parallel configuration integrating a linear motor with a damper.

Preview control, as an advanced suspension control strategy, requires precise road identification. Inter-axle preview, which utilizes the dynamic performance of the front wheels as a reference, has relatively high feasibility and practicability. Model predictive control is suitable for controlling suspension systems as it can explicitly handle disturbances.[6,7]

This paper investigates the establishment of a four-degree-of-freedom dynamic model of a 1/2 vehicle body with energy-regenerative suspension, imports the road input model for simulation, and examines the energy-regenerative efficiency of the suspension. [8]Based on the inter-axle preview strategy, the model predictive control is optimized to establish the inter-axle predictive control method. Simulation to verify the performance of the system.

2. Four-Degree-of-Freedom 1/2 vehicle Suspension Dynamics Model

The study of suspension properties is often based on the vehicle body vibration model. The dynamics performance of the vehicle vertical system is typically investigated by resorting to three classic vehicle body models: the 1/4 vehicle body two-degree-of-freedom model, the 1/2 vehicle body four-degree-of-freedom model, and the full vehicle seven-degree-of-freedom model. Under the assumption of no lateral tilt and steering on a straight road, the 1/2 vehicle body four-degree-of-freedom model can reflect the vertical vibration and pitch vibration characteristics of the vehicle. It not only meets the design verification requirements and can accurately predict the vehicle's driving vibration characteristics but also avoids excessive complexity and additional design burden.

Firstly, assumptions regarding the physical state of the suspension system are made as follows:

(1) The linear actuator is regarded as an idealized force involved in the model. The mass of the motor is combined with the vehicle body. In the energy-regenerative mode, it participates in the calculation in the form of damping force, and in the active control mode, it participates in the calculation as an active actuating force.

(2) All masses are considered as rigid bodies.

(3) Only road roughness is considered as the system input, while other vibration sources of the vehicle body are disregarded.

(4) Due to the minor influence of tire damping, its effect on the system is neglected.

(5) Considering the straight driving condition, the road has no camber.

The schematic diagram of the 1/2 vehicle body four-degree-of-freedom suspension system dynamics model is presented as Figure 1.

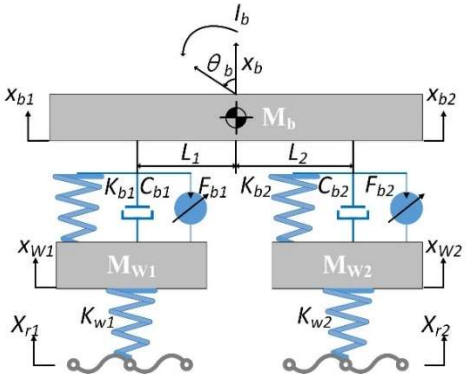

Figure 1. 1/2 vehicle body four-degree-of-freedom suspension system dynamics model

ISSN: 2710-0723

In the figure: K_{b1} and K_{b2} denote the stiffness of the front and rear shock absorbers; K_{w1} and K_{w2} denote the stiffness of the front and rear wheels; C_{b1} and C_{b2} denote the damping coefficients of the front and rear shock absorbers; F_{b1} and F_{b2} denote the electromagnetic force or positioning force of the front and rear motors; x_{r1} and x_{r2} denote the road input beneath the front and rear wheels; x_{w1} and x_{w2} denote the vertical displacement of the front and rear unsprung masses; x_b represents the vertical displacement of the center of gravity of the sprung mass; x_{b1} and x_{b2} represent the displacements of the front and rear ends of the unsprung mass; L_1 and L_2 represent the distances from the front and rear ends of the unsprung mass to the center of gravity; θ_b represents the pitch angle of the sprung mass; I_b represents the pitch moment of inertia of the sprung mass.

Taking into account the vertical acceleration of the center of mass of the sprung mass, the pitch angular acceleration of the sprung mass, and the vertical acceleration of the unsprung mass, the motion differential equation of the model is analyzed in accordance with Newton's second law as follows:

$$\begin{cases} M_b\ddot{x}_b = K_{b1}(x_{W1}-x_{b1})+C_{b1}(\dot{x}_{W1}-\dot{x}_{b1})+F_{b1}+K_{b2}(x_{W2}-x_{b2})+C_{b2}(\dot{x}_{W2}-\dot{x}_{b2})+F_{b2} \\ M_{W1}\ddot{x}_{W1} = K_{b1}(x_{b1}-x_{W1})+C_{b1}(\dot{x}_{b1}-\dot{x}_{W1})-K_{W1}(x_{W1}-x_{r1})-F_{b1} \\ M_{W2}\ddot{x}_{W2} = K_{b2}(x_{b2}-x_{W2})+C_{b2}(\dot{x}_{b2}-\dot{x}_{W2})-K_{W2}(x_{W2}-x_{r2})-F_{b2} \\ I_b\ddot{\theta}_b = L_1\left(K_{b1}\left(x_{b1}-x_{W1}\right)+C_{b1}\left(\dot{x}_{b1}-\dot{x}_{W1}\right)-F_{b1}\right) \\ \qquad -L_2\left(K_{b2}\left(x_{b2}-x_{W2}\right)+C_{b2}\left(\dot{x}_{b2}-\dot{x}_{W2}\right)-F_{b2}\right) \\ x_{b1} = x_b - L_1\theta_b \\ x_{b2} = x_b - L_2\theta_b \end{cases} \tag{1}$$

The system state-space equations can be mathematically formulated as follows:

$$\begin{cases} \dot{\mathrm{X}}=\mathrm{AX}+\mathrm{BF}+\mathrm{EW} \\ \mathrm{Y}=\mathrm{CX}+\mathrm{DF} \end{cases} \tag{2}$$

The matrices in the formula are as follows:

$$A=\begin{bmatrix} -\frac{C_{b1}+C_{b2}}{M_b} & \frac{L_1C_{b1}-L_2C_{b2}}{M_b} & \frac{C_{b1}}{M_b} & \frac{C_{b2}}{M_b} & \frac{-K_{b1}}{M_b} & \frac{-K_{b2}}{M_b} & 0 & 0 \\ \frac{L_1C_{b1}-L_2C_{b2}}{I_b} & \frac{L_1^{\,2}C_{b1}+L_2^{\,2}C_{b2}}{I_b} & \frac{-L_1C_{b1}}{I_b} & \frac{L_2C_{b2}}{I_b} & \frac{L_1K_{b1}}{I_b} & \frac{-L_2K_{b2}}{I_b} & 0 & 0 \\ \frac{C_{b1}}{M_{W1}} & \frac{-L_1C_{b1}}{M_{W1}} & \frac{-C_{b1}}{M_{W1}} & 0 & \frac{K_{b1}}{M_{W1}} & 0 & \frac{-K_{W1}}{M_{W1}} & 0 \\ \frac{C_{b2}}{M_{W2}} & \frac{L_2C_{b2}}{M_{W2}} & 0 & \frac{-C_{b2}}{M_{W2}} & 0 & \frac{K_{b2}}{M_{w2}} & 0 & \frac{-K_{W2}}{M_{w2}} \\ 1 & -L_1 & -1 & 0 & 0 & 0 & 0 & 0 \\ 1 & L_2 & 0 & -1 & 0 & 0 & 0 & 0 \\ 0 & 0 & 1 & 0 & 0 & 0 & 0 & 0 \\ 0 & 0 & 0 & 1 & 0 & 0 & 0 & 0 \end{bmatrix} \tag{3}$$

ISSN: 2710-0723

$$B=\begin{bmatrix} \frac{1}{M_b} & \frac{1}{M_b} \\ \frac{-L_1}{I_b} & \frac{L_2}{I_b} \\ \frac{-1}{M_{b1}} & 0 \\ 0 & \frac{-1}{M_{b2}} \\ 0 & 0 \\ 0 & 0 \\ 0 & 0 \\ 0 & 0 \end{bmatrix};\quad E=\begin{bmatrix} 0 & 0 \\ 0 & 0 \\ 0 & 0 \\ 0 & 0 \\ 0 & 0 \\ 0 & 0 \\ -1 & 0 \\ 0 & -1 \end{bmatrix};\quad D=\begin{bmatrix} \frac{1}{M_b} & \frac{1}{M_b} \\ \frac{-L_1}{I_b} & \frac{L_2}{I_b} \\ 0 & 0 \\ 0 & 0 \\ 0 & 0 \\ 0 & 0 \end{bmatrix} \tag{4}$$

$$C=\begin{bmatrix} -\frac{C_{b1}+C_{b2}}{M_b} & \frac{L_1C_{b1}-L_2C_{b2}}{M_b} & \frac{C_{b1}}{M_b} & \frac{C_{b2}}{M_b} & \frac{-K_{b1}}{M_b} & \frac{-K_{b2}}{M_b} & 0 & 0 \\ \frac{L_1C_{b1}-L_2C_{b2}}{I_b} & \frac{L_1^2C_{b1}+L_2^2C_{b2}}{I_b} & \frac{-L_1C_{b1}}{I_b} & \frac{L_2C_{b2}}{I_b} & \frac{L_1K_{b1}}{I_b} & \frac{-L_2K_{b2}}{I_b} & 0 & 0 \\ 0 & 0 & 0 & 0 & 1 & 0 & 0 & 0 \\ 0 & 0 & 0 & 0 & 0 & 1 & 0 & 0 \\ 0 & 0 & 0 & 0 & 0 & 0 & 1 & 0 \\ 0 & 0 & 0 & 0 & 0 & 0 & 0 & 1 \end{bmatrix} \tag{5}$$

3. Inter-Axle Preview-Enhanced Model Predictive Control for Energy-Regenerative Suspension Systems

In this paper, a transverse flux motor is employed as the active actuator and vibration energy harvester of the suspension. This energy-regenerative suspension is capable of recovering vibration energy and simultaneously can serve as an active actuator to restrain the vibration of the vehicle body. Hence, it can strike a balance between active control and energy conservation through a self-powered approach. The principle of the self-powered mode is depicted as Figure 2.

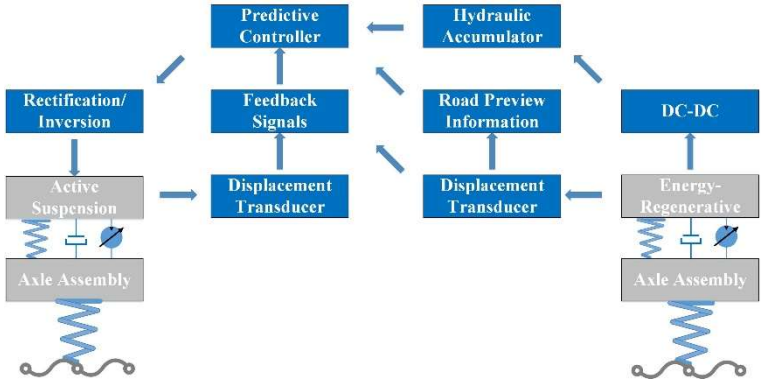

Figure 2. The principle of the self-powered mode

ISSN: 2710-0723

The state space equation of the continuous system for the vertical dynamics model of the quarter-car four-degree-of-freedom suspension has been presented previously. For the implementation of model predictive control, the discretization of the state space equation is required, which can be obtained using the forward Euler method.

The forward Euler method is an explicit numerical integration approach employed to discretize the continuous-time differential equation into a difference equation. Through the linear approximation prediction method, the state at the next moment is predicted. If the sampling time is T_S, the differential term in the continuous state equation is as follows:

$$\frac{dX}{dt} \approx \frac{X[k+1]-X[k]}{T_S} \tag{6}$$

Substituted into the continuous equation of the system state, the equation is as follows:

$$\frac{X[k+1]-X[k]}{T_S} = AX[k]+BF[k]+EW[k] \tag{7}$$

It is organized in the following form:

$$X[k+1] = (I+T_sA)X[k]+T_sBF[k]+T_sEW[k] \tag{8}$$

From the organized form, the original system state equation can be denoted as follows:

$$\begin{cases} \mathrm{X}_{k+1}=\mathrm{A}^{*}\mathrm{X}_{k}+\mathrm{B}^{*}\mathrm{F}_{k}+\mathrm{E}^{*}\mathrm{W}_{k} \\ \mathrm{Y}_{k}=\mathrm{CX}_{k}+\mathrm{DF}_{k} \end{cases} \tag{9}$$

The prediction horizon is defined as N_{p} and the control horizon as N_{c}. Then, the system control sequence, state variables, output variables, and input are as follows:

$$\begin{cases} \hat{F} = [F_k, F_{k+1}, \cdots F_{k+N_c}]^T \\ \hat{X} = [X_k, X_{k+1}, \cdots X_{k+N_p}]^T \\ \hat{Y} = [Y_k, Y_{k+1}, \cdots Y_{k+N_p}]^T \\ \hat{W} = [W_k, W_{k+1}, \cdots W_{k+N_p-1}]^T \end{cases} \tag{10}$$

By recursively unfolding the state equation, a linear combination of the initial state and the control sequence can be obtained as follows:

ISSN: 2710-0723

$$
\begin{aligned}
&X_{k+1}=A^{*}X_{k}+B^{*}F_{k}+E^{*}W_{k}\\
&X_{k+2}=\left(A^{*}\right)^{2}X_{k}+A^{*}B^{*}F_{k}+B^{*}F_{k+1}+A^{*}E^{*}W_{k}+E^{*}W_{k+1}\\
&\vdots\\
&\vdots\\
&X_{k+N_{\mathrm{p}}}=\left(A^{*}\right)^{N_{\mathrm{p}}}X_{k}+\left(A^{*}\right)^{N_{p}-1}B^{*}F_{k}+\left(A^{*}\right)^{N_{p}-2}B^{*}F_{k+1}\cdots+\sum_{i=1}^{N_{p}-N_{c}}\left(A^{*}\right)^{i-1}B^{*}F_{k+N_{c}}+\cdots\\
&+\left(A^{*}\right)^{N_{p}}E^{*}W_{k}+\left(A^{*}\right)^{N_{p}-1}E^{*}W_{k+1}+\cdots+E^{*}W_{k+N_{p}-1}
\end{aligned}
\tag{11}
$$

The stacking is arranged in matrix form as follows:

$$
\begin{aligned}
\hat{X}=&\begin{bmatrix}\left(A^{*}\right)\\ \left(A^{*}\right)^{2}\\ \vdots\\ \left(A^{*}\right)^{N_{\mathrm{p}}}\end{bmatrix}X_{k}+\begin{bmatrix}B^{*} & 0 & \cdots & 0\\ \left(A^{*}\right)B^{*} & B^{*} & \cdots & 0\\ \vdots & \vdots & \ddots & \vdots\\ \left(A^{*}\right)^{N_{p}-1}B^{*} & \left(A^{*}\right)^{N_{p}-2}B^{*} & \cdots & \sum_{i=1}^{N_{p}-N_{c}}\left(A^{*}\right)^{i-1}B^{*}\end{bmatrix}\hat{F}\\
&+\begin{bmatrix}E^{*} & 0 & \cdots & 0\\ \left(A^{*}\right)E^{*} & E^{*} & \cdots & 0\\ \vdots & \vdots & \ddots & \vdots\\ \left(A^{*}\right)^{N_{p}-1}E^{*} & \left(A^{*}\right)^{N_{p}-2}E^{*} & \cdots & E^{*}\end{bmatrix}\hat{W}
\end{aligned}
\tag{12}
$$

The compact form of the discrete equation for the predicted state can be derived as follows:

$$\hat{X}=\Psi X_{k}+\Phi\hat{F}+\Gamma\hat{W} \tag{13}$$

Similarly, through recursive expansion of the output equation, the following linear combination can be attained:

$$
\begin{aligned}
&Y_{k+1}=CA^{*}X_{k}+CB^{*}F_{k}+CE^{*}W_{k}+DF_{k+1}\\
&Y_{k+2}=C\left(A^{*}\right)^{2}X_{k}+CA^{*}B^{*}F_{k}+CB^{*}F_{k+1}+CA^{*}E^{*}W_{k}+CE^{*}W_{k+1}+DF_{k+2}\\
&\vdots\\
&\vdots\\
&Y_{k+N_{\mathrm{p}}}=C\left(A^{*}\right)^{N_{\mathrm{p}}}X_{k}+C\left(A^{*}\right)^{N_{p}-1}B^{*}F_{k}+\cdots+\left(\sum_{i=1}^{N_{p}-N_{c}}\left(A^{*}\right)^{i-1}B^{*}+D\right)F_{k+N_{c}}+\cdots\\
&+C\left(A^{*}\right)^{N_{p}}E^{*}W_{k}+C\left(A^{*}\right)^{N_{p}-1}E^{*}W_{k+1}+\cdots+CE^{*}W_{k+N_{p}-1}
\end{aligned}
\tag{14}
$$

The stacking is arranged in matrix form as follows:

ISSN: 2710-0723

$$\hat{\mathrm{Y}}=\begin{bmatrix}\mathrm{C}\left(\mathrm{A}^{*}\right)\\ \mathrm{C}\left(\mathrm{A}^{*}\right)^{2}\\ \vdots\\ \mathrm{C}\left(\mathrm{A}^{*}\right)^{N_{\mathrm{p}}}\end{bmatrix}\mathrm{X}_{k}+\begin{bmatrix}\mathrm{CB}^{*} & \mathrm{D} & 0 & \cdots & 0\\ \mathrm{C}\left(\mathrm{A}^{*}\right)\mathrm{B}^{*} & \mathrm{CB}^{*} & \mathrm{D} & \cdots & 0\\ \vdots & \vdots & \vdots & \ddots & \vdots\\ \mathrm{C}\left(\mathrm{A}^{*}\right)^{N_{\mathrm{p}}-1}\mathrm{B}^{*} & \mathrm{C}\left(\mathrm{A}^{*}\right)^{N_{\mathrm{p}}-2}\mathrm{B}^{*} & \cdots & \cdots & \sum_{i=1}^{N_p-N_c}\mathrm{C}\left(\mathrm{A}^{*}\right)^{i-1}\mathrm{B}^{*}+\mathrm{D}\end{bmatrix}\hat{\mathrm{F}}$$
$$+\begin{bmatrix}\mathrm{CE}^{*} & 0 & \cdots & 0\\ \mathrm{C}\left(\mathrm{A}^{*}\right)\mathrm{E}^{*} & \mathrm{CE}^{*} & \cdots & 0\\ \vdots & \vdots & \ddots & \vdots\\ \mathrm{C}\left(\mathrm{A}^{*}\right)^{N_p-1}\mathrm{E}^{*} & \mathrm{C}\left(\mathrm{A}^{*}\right)^{N_p-2}\mathrm{E}^{*} & \cdots & \mathrm{CE}^{*}\end{bmatrix}\hat{\mathrm{W}} \tag{15}$$

The compact form of the complete prediction equation can be derived as follows:

$$\begin{cases}\hat{\mathrm{X}}=\Psi_{X}\mathrm{X}_{k}+\Phi_{X}\hat{\mathrm{F}}+\Gamma_{X}\hat{\mathrm{W}}\\ \hat{\mathrm{Y}}=\Psi_{Y}\mathrm{X}_{k}+\Phi_{Y}\hat{\mathrm{F}}+\Gamma_{Y}\hat{\mathrm{W}}\end{cases} \tag{16}$$

Based on the system dynamics equation, if the system output is the main controlled object, then taking the system output and the active control input as the controlled objects, the cost function is established as follows:

$$J=\sum_{i=1}^{N_p}{Y_{k+i}}^{T}QY_{k+i}+\sum_{j=0}^{N_p}{F_{k+j}}^{T}RF_{k+j} \tag{17}$$

The objective function is simplified to a quadratic cost function. The compact form of the prediction equation is substituted into the cost function as follows:

$$\begin{aligned}J&=\left(\Psi_{Y}\mathrm{X}_{k}+\Phi_{Y}\hat{\mathrm{F}}+\Gamma_{Y}\hat{\mathrm{W}}\right)^{T}Q\left(\Psi_{Y}\mathrm{X}_{k}+\Phi_{Y}\hat{\mathrm{F}}+\Gamma_{Y}\hat{\mathrm{W}}\right)+\hat{\mathrm{F}}^{T}R\hat{\mathrm{F}}\\ &=\mathrm{X}_{k}{}^{T}\Psi_{Y}{}^{T}Q\Psi_{Y}\mathrm{X}_{k}+\hat{\mathrm{F}}^{T}\Phi_{Y}{}^{T}Q\Phi_{Y}\hat{\mathrm{F}}\\ &+\hat{\mathrm{W}}^{T}\Gamma_{Y}{}^{T}Q\Gamma_{Y}\hat{\mathrm{W}}+2\mathrm{X}_{k}{}^{T}\Psi_{Y}{}^{T}Q\Gamma_{Y}\hat{\mathrm{W}}\\ &+2\mathrm{X}_{k}{}^{T}\Psi_{Y}{}^{T}Q\Phi_{Y}\hat{\mathrm{F}}+2\hat{\mathrm{W}}^{T}\Gamma_{Y}{}^{T}Q\Phi_{Y}\hat{\mathrm{F}}+\hat{\mathrm{F}}^{T}R\hat{\mathrm{F}}\end{aligned} \tag{18}$$

Since the control input is the control force F, the cost function can be linearly combined into the following form:

$$\begin{aligned}J&=\hat{\mathrm{F}}^{T}\left(\Phi_{Y}{}^{T}Q\Phi_{Y}+R\right)\hat{\mathrm{F}}+2\left(\mathrm{X}_{k}{}^{T}\Psi_{Y}{}^{T}Q\Phi_{Y}+\hat{\mathrm{W}}^{T}\Gamma_{Y}{}^{T}Q\Phi_{Y}\right)\hat{\mathrm{F}}\\ &+\mathrm{X}_{k}{}^{T}\Psi_{Y}{}^{T}Q\Psi_{Y}\mathrm{X}_{k}+\hat{\mathrm{W}}^{T}\Gamma_{Y}{}^{T}Q\Gamma_{Y}\hat{\mathrm{W}}+2\mathrm{X}_{k}{}^{T}\Psi_{Y}{}^{T}Q\Gamma_{Y}\hat{\mathrm{W}}\end{aligned} \tag{19}$$

The quadratic programming formulation can be mathematically expressed in the following:

ISSN: 2710-0723

$$\min_{\hat{F}} \boldsymbol{J} = \hat{\boldsymbol{F}}^{T}\boldsymbol{H}\hat{\boldsymbol{F}}+2\boldsymbol{g}\hat{\boldsymbol{F}}+\boldsymbol{C}_{t} \tag{20}$$

The preview time τ can be approximated as the ratio of wheelbase to vehicle speed. The road input transfer function with a delay equivalent to one wheelbase is expressed as:

$$\frac{W_2(s)}{W_1(s)} = e^{-\tau s} \approx \frac{1-\frac{\tau s}{2}+\frac{(\tau s)^2}{8}}{1+\frac{\tau s}{2}+\frac{(\tau s)^2}{8}} \tag{21}$$

The time-domain expression is constructed using the Padé approximation method, and the output equation is formulated as:

$$W_2(s) = \eta(t) - W_1(s) \tag{22}$$

The state-space equation is established as:

$$\dot{\eta}(t) = \begin{bmatrix} 0 & 1 \\ -\frac{8}{\tau^2} & -\frac{4}{\tau} \end{bmatrix} \begin{bmatrix} \eta_1 \\ \eta_2 \end{bmatrix} + \begin{bmatrix} -\frac{8}{\tau} \\ \frac{32}{\tau^2} \end{bmatrix} W_1(t) = A_\eta \eta(t) + B_\eta W_1(t) \tag{23}$$

By integrating the preview information into the system state equation, the augmented state equation is derived as:

$$\begin{bmatrix} \dot{X} \\ \dot{\eta} \end{bmatrix} = \begin{bmatrix} A & ED_\eta \\ 0 & A_\eta \end{bmatrix} \begin{bmatrix} X \\ \eta \end{bmatrix} + \begin{bmatrix} B \\ 0 \end{bmatrix} F + \begin{bmatrix} EI_\eta \\ B_\eta \end{bmatrix} w_1 \tag{24}$$

When the system input is deterministic, the reference output can be constructed based on the current system state and predicted input over the preview horizon, where the disturbance input within the prediction horizon becomes a priori known quantity.

Let $\mathrm{X}_{\mathrm{ref(k)}}$ denote the reference state at time step k, and $\hat{\mathrm{Y}}_{\mathrm{ref(k)}}$ represent the reference output. The error formulation is then defined as:

$$\begin{cases} \hat{\mathrm{E}}_{\mathrm{k}} = \Psi_Y \mathrm{X}_{\mathrm{k}} - \Psi_Y \mathrm{X}_{\mathrm{ref(k)}} \\ \hat{\mathrm{Y}}_{\mathrm{k}} - \hat{\mathrm{Y}}_{\mathrm{ref(k)}} = \hat{E}_{\mathrm{k}} + \Phi_Y \hat{\mathrm{F}} \end{cases} \tag{25}$$

4. Simulation Results and Analysis

Intelligent vehicles boast rich application scenarios and flexible structural designs. Currently, rather strict or universal industrial standards and national standards are lacking. In the general consumer market, civilian scenarios, and research, intelligent vehicles typically take the form of light electric vehicles, equipped with superior information processing units and an abundance of sensors. Numerous research teams have carried out diverse studies on intelligent

ISSN: 2710-0723

vehicles and fabricated many prototypes featuring intelligent vehicle functions or technologies. According to the common vehicle parameters in the current market and the parameters of some intelligent vehicle research prototypes, the relevant simulation parameters of the intelligent vehicle suspension system are selected and presented in Table 1.

Table 1. the relevant simulation parameters of the intelligent vehicle suspension system

Parameter	Symbol	Value	Unit
Sprung Mass	M_b	1160	kg
Unsprung Mass	M_W	41.5	kg
Suspension Spring Rate	K_b	27000	N/m
Tire Vertical Stiffness	K_w	200000	N/m
Damper Damping Coefficient	C_b	1226	N•s/m
Distance from Front Axle to Center of Gravity	L_1	1.26	m
Distance from Rear Axle to Center of Gravity	L_2	1.158	m
Vehicle Pitch Moment of Inertia	I_b	1622	Kg•m2

In order to investigate the effectiveness of the control system, applying a compound road excitation to the system input enables obtaining the efficacy of the suspension in the control system under various circumstances. This paper sets a compound road excitation composed of a C-level road and a D-level road, and assumes that the vehicle operates for 20 seconds, running on the C-level road for the first 10 seconds and on the D-level road thereafter. The compound road excitation curve is shown as in Figure 3.

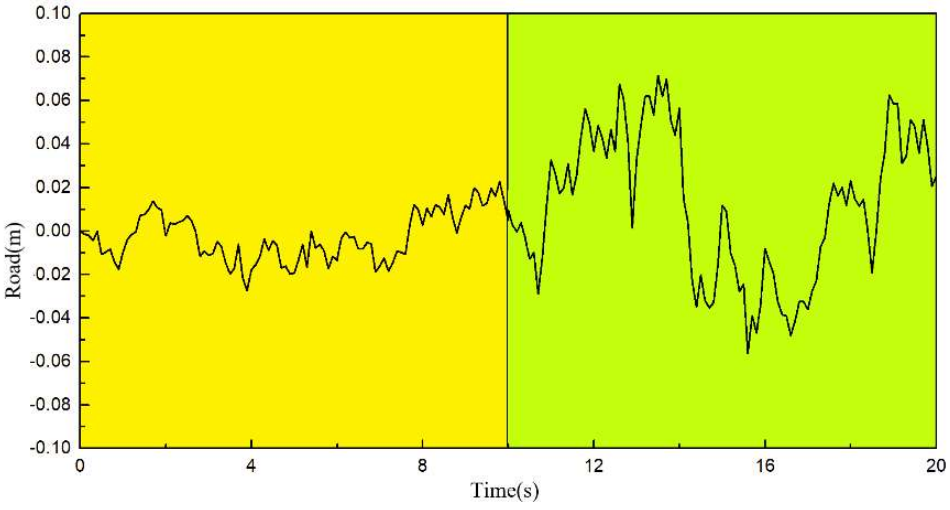

Figure 3. The compound road excitation curve

The road surface excitation is input into the vehicle suspension system dynamics model for simulation. The output vector data is exported for comparison.

Pitch Angular Acceleration can explain the dynamic response of the vehicle when it receives road impact. The comparison of simulation results under the two modes is shown in the Figure 4.

ISSN: 2710-0723

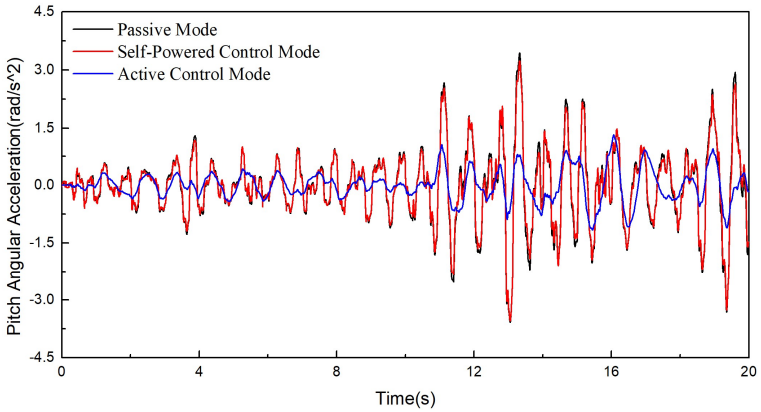

Figure 4. Comparison of simulation results of Pitch Angular Acceleration

Wheel Dynamic Load can explain the contact performance between the vehicle and the ground. As an important indicator of vehicle safety, it has research value. Comparison of simulation results of Front Wheel Dynamic Load is shown in Figure 5. Comparison of simulation results of Rear Wheel Dynamic Load is shown in Figure 6.

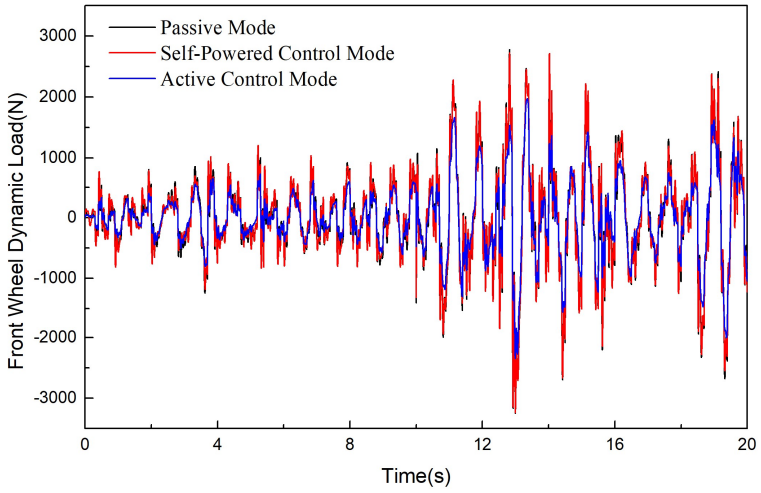

Figure 5. Comparison of simulation results of Front Wheel Dynamic Load

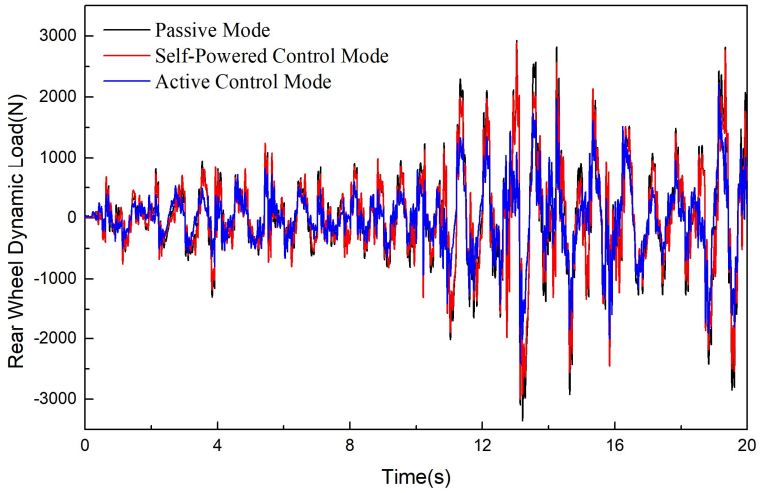

Figure 6. Comparison of simulation results of Rear Wheel Dynamic Load

ISSN: 2710-0723

Vertical Acceleration can directly indicate passengers' feeling of road impact and is an important indicator for evaluating comfort. The comparison of Vertical Acceleration can show the impact intensity felt by passengers in different modes. Acceleration Power Spectral Density can further illustrate the suppression effect of different modes on impact intensity in different frequency ranges.

Comparison of simulation results of Vertical Acceleration is shown in Figure 7(a). Comparison of simulation results of Acceleration Power Spectral Density is shown in Figure 7(b).

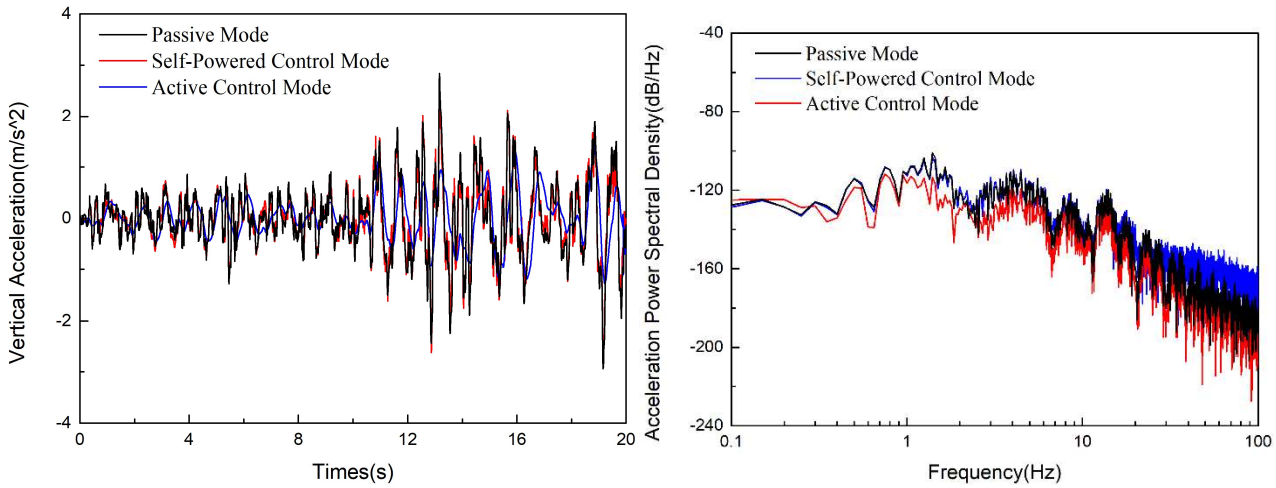

(a)Vertical Acceleration (b) Acceleration Power Spectral Density

Figure 7. Comparison of simulation results of Vertical Acceleration and Acceleration Power Spectral Density

The instantaneous power of the vibration energy harvester in the energy regenerative suspension is shown in Figure 8.

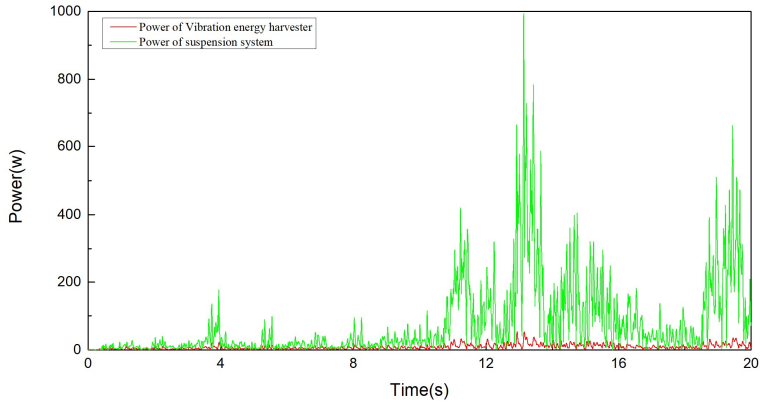

Figure 8. Comparison of simulation results of The instantaneous power

To compare system parameters under different modes, root mean square values of simulation results are calculated and compared. The results show that Compared to Passive Mode, Active Control Mode achieves:

(1)43.92% optimization in Pitch Angular Acceleration.

(2)24.71% and 36.61% optimizations in Wheel Dynamic Load (front and rear, respectively).

(3)33.85% optimization in Vertical Acceleration intensity within the human-sensitive frequency range.

ISSN: 2710-0723

This indicates that the suspension system under active control effectively improves vehicle dynamic performance.

In Self-Powered Control Mode, the vehicle body technical parameters are optimized by 2.54%, 3.21%, and 4.68%, respectively. This demonstrates that the suspension system can still moderately enhance vehicle dynamic performance even without external energy input.

Compared to the energy passively dissipated by the suspension system, the instantaneous power of the vibration energy harvester is approximately 11.06% of the suspension system's dissipated power. This proves that the energy-regenerative suspension can effectively recover vibration energy.

5. Conclusion

This paper discusses an active control method for energy-regenerative suspension systems. The system integrates active actuators and vibration energy harvesters, which can either recover energy from road-induced vibrations or actively suppress vibrations. By employing a preview method-enhanced model predictive control, the dynamic performance of the suspension system is effectively improved. Simulation analyses demonstrate that:

(1)In Active Control Mode, both safety and comfort performance metrics of the suspension system are significantly enhanced.

(2)In Self-Powered Control Mode, the suspension system still achieves moderate performance improvements without requiring any additional energy input from the vehicle.

(3)Compared to conventional suspension systems, the vibration energy harvester in the energy-regenerative suspension system effectively recovers vibrational energy.

This paper provides a reference for the application of model predictive control in suspension systems. The study on energy-regenerative suspension systems holds significant potential and value for further in-depth research.

Acknowledgments

The authors declared that this study has received no financial support.

The authors have no conflict of interest to declare.

References

[1] Y. Zhao, Y. Zhang, L. Guo, S. Ding and X. Wang: Advances in Machine Learning-Based Active Vibration Control for Automotive Seat Suspensions: A Comprehensive Review, Mechanical Systems and Signal Processing, Vol. 231 (2025) No.5, p.112645.

[2] L. Pang, M. Yue, G. Qi, Y. Liu and K. Qian: Preview-Based MPC for Active Suspension Control of Tank Vehicle with Lateral Liquid Sloshing Suppression, Proceedings of the Institution of Mechanical Engineers Part D-Journal of Automobile Engineering, (2025), DOI:10.1177/09544070251317649.

[3] S. Wen, M. Chen, Z. Zeng, X. Yu and T. Huang: Fuzzy Control for Uncertain Vehicle Active Suspension Systems via Dynamic Sliding-Mode Approach, IEEE Transactions on Systems Man Cybernetics-Systems, Vol. 47 (2017) No.1, p.24-32.

[4] P. Liu, F. Kou, Y. Chen, G. Wang and L. Xing: Modeling and Dynamic Analysis of a Novel Energy-Regenerative Hydraulically Interconnected Suspension, Energy, Vol. 324 (2025), p.135928.

[5] S. Yan and W. Sun: Self-Powered Suspension Criterion and Energy Regeneration Implementation Scheme of Motor-Driven Active Suspension, Mechanical Systems and Signal Processing, Vol. 94 (2017), p.297-311.

[6] G. Wang, F. Kou, P. Liu, W. Lv and L. Xing: Road Preview Method for Active Suspension Based on Reinforcement Learning, Measurement Science and Technology, Vol. 36 (2025) No.3, p.036206.

ISSN: 2710-0723

[7] P. Li, J. Lam and K. Cheung: Multi-Objective Control for Active Vehicle Suspension with Wheelbase Preview, Journal of Sound and Vibration, Vol. 333 (2014) No.21, p.5269-5282.

[8] P. Bazios, F. Khoshnoud and I. Esat: Energy Harvesting from Suspension System and Self-Powered Vibration Control for a Seven Degree of Freedom Vehicle Model, Proceedings of the Institution of Mechanical Engineers Part K-Journal of Multi-Body Dynamics, Vol. 232 (2018) No.3, p.342-356.